

The spatial and temporal complexity of the Holocene thermal maximum

H. Renssen^{1*}, H. Seppä², O. Heiri³, D. M. Roche⁴, H. Goosse⁵ and T. Fichetfot⁵

The Holocene thermal maximum, a period of relatively warm climate between 11,000 and 5,000 years ago^{1,2}, is most clearly recorded in the middle and high latitudes^{2,3} of the Northern Hemisphere, where it is generally associated with the local orbitally forced summer insolation maximum. However, proxy-based reconstructions have shown that both the timing and magnitude of the warming vary substantially between different regions²⁻⁴, suggesting the involvement of extra feedbacks and forcings. Here, we simulate the Holocene thermal maximum in a coupled global ocean-atmosphere-vegetation model. We find that before 7,000 years ago, summers were substantially cooler over regions directly influenced by the presence of the Laurentide ice sheet, whereas other regions of the Northern Hemisphere were dominated by orbital forcing. Our simulations suggest that the cool conditions arose from a combination of the inhibition of Labrador Sea deep convection by the flux of meltwater from the ice sheet, which weakened northward heat transport by the ocean, and the high surface albedo of the ice sheet. We thus conclude that interglacial climate is highly sensitive to relatively small changes in ice-sheet configuration.

In this study, we analyse the temporal and spatial structure of the Holocene thermal maximum (HTM) in the Northern Hemisphere in coupled climate model simulations and high-quality quantitative proxy-based climate reconstructions. Previous transient climate model simulations driven by orbital and greenhouse gas forcing have been unable to capture the variation in HTM timing^{5,6}. One important factor that was missing in these model studies is the influence of deglaciation^{7,8}. Although the Holocene formally starts after the termination of the Younger Dryas cold phase at 11.7 kyr BP (ref. 9), the deglaciation of the large 'glacial' ice sheets in North America and Eurasia continued for several millennia after the Younger Dryas/Holocene transition¹⁰. The Fennoscandian ice sheet persisted until 9 kyr BP (ref. 11), and the last substantial remnants of the Laurentide ice sheet (LIS) vanished as late as 7 kyr BP (ref. 12). These early Holocene ice sheets can be expected to have had a cooling effect at least at the regional scale, thereby compensating for the relatively strong orbitally forced insolation in summer¹³. Indeed, the LIS clearly is responsible for a delayed HTM in northeast Canada between 7 and 6 kyr BP, strongly contrasting with the timing of maximum warmth in Alaska and northwest Canada that is synchronous with the orbital-induced summer insolation maximum between 11 and 9 kyr BP (ref. 4). The impact of the LIS on climatic conditions outside North America has remained as yet unclear.

To study the impact of LIS deglaciation on the circumpolar Holocene climate, we have carried out five transient climate

model simulations (see Table 1) covering the past 9,000 years with the ECBilt-CLIO-VECODE model¹⁴⁻¹⁶, which is a global atmosphere-ocean-vegetation model of intermediate complexity (see the Methods section and Supplementary Information).

Considering the temperature response at the scale of the Arctic, orbital forcing is the dominant long-term forcing over the whole Holocene, whereas the effect of variations in atmospheric greenhouse gases is minor (Fig. 1a). In experiment ORB, summer temperatures north of 60° N were 2 °C warmer at 9 kyr BP than at 0 kyr. The effect of greenhouse gas forcing alone is a slight warming (0.3 °C) over the past 9 kyr. The LIS meltwater flux and the presence of the remnant LIS both have a cooling effect on the early Holocene climate before 7 kyr (Fig. 1a), effectively counteracting the influence of orbital forcing and delaying the thermal maximum by two millennia at the scale of the Arctic. However, even in the experiment including the full LIS influence (OGMELTICE), the early Holocene (9 kyr BP) was still warmer than at 0 kyr. After 7 kyr BP, summer temperatures closely follow orbital forcing.

The background LIS meltwater flux freshens the surface ocean, particularly in the northwest Atlantic. As a result, deep convection in the Labrador Sea is no longer active in OGMELT between 9.0 and 7.8 kyr BP in contrast to ORBGHG. This leads to a slightly weakened overturning circulation, with North Atlantic Deep Water export at 30° S decreasing from 13.5 Sv in ORBGHG to 10.5 Sv in OGMELT, and reduced northward heat transport by the Atlantic Ocean from 0.32 PW at 20° S in ORBGHG to 0.23 PW in OGMELT. As a consequence, surface cooling and sea-ice expansion take place in the northwest Atlantic and the Labrador Sea becomes perennially ice-covered in OGMELT (Fig. 2a, b). At the scale of the Arctic, summers are 0.5 °C cooler compared with ORBGHG (Fig. 1a).

Table 1 | Summary of experiments discussed in this letter.

Experiment name	Forcings
ORB	Orbital
GHG	CO ₂ and CH ₄
ORBGHG	Orbital, CO ₂ and CH ₄
OGMELT	As ORBGHG, plus LIS background meltflux
OGMELTICE	As OGMELT, plus LIS surface albedo and topography

The ORB and GHG simulations represent the separate responses to orbital²⁶ and greenhouse gas²⁷ forcing, respectively, whereas experiment ORBGHG combines these two forcings. Simulation OGMELT includes an extra freshwater forcing describing the LIS background meltflux¹⁹. Experiment OGMELTICE also includes the LIS topography and surface albedo¹⁰ (see Supplementary Information) and thus describes the total response to all considered forcings.

¹Department of Earth Sciences, Faculty of Earth and Life Sciences, VU University Amsterdam, NL-1081HV Amsterdam, The Netherlands, ²Department of Geology, University of Helsinki, Helsinki FI-00014, Finland, ³Palaeoecology, Institute of Environmental Biology, Utrecht University, NL-3584 CD Utrecht, The Netherlands, ⁴Laboratoire des Sciences du Climat et de l'Environnement (LSCE/IPSL), Laboratoire CEA/INSU-CNRS/UVSQ, Gif sur Yvette Cedex F-91191, France, ⁵Institut d'Astronomie et de Géophysique G. Lemaître, Université Catholique de Louvain, Louvain-la-Neuve B-1348, Belgium.

*e-mail: hans.rensen@falw.vu.nl

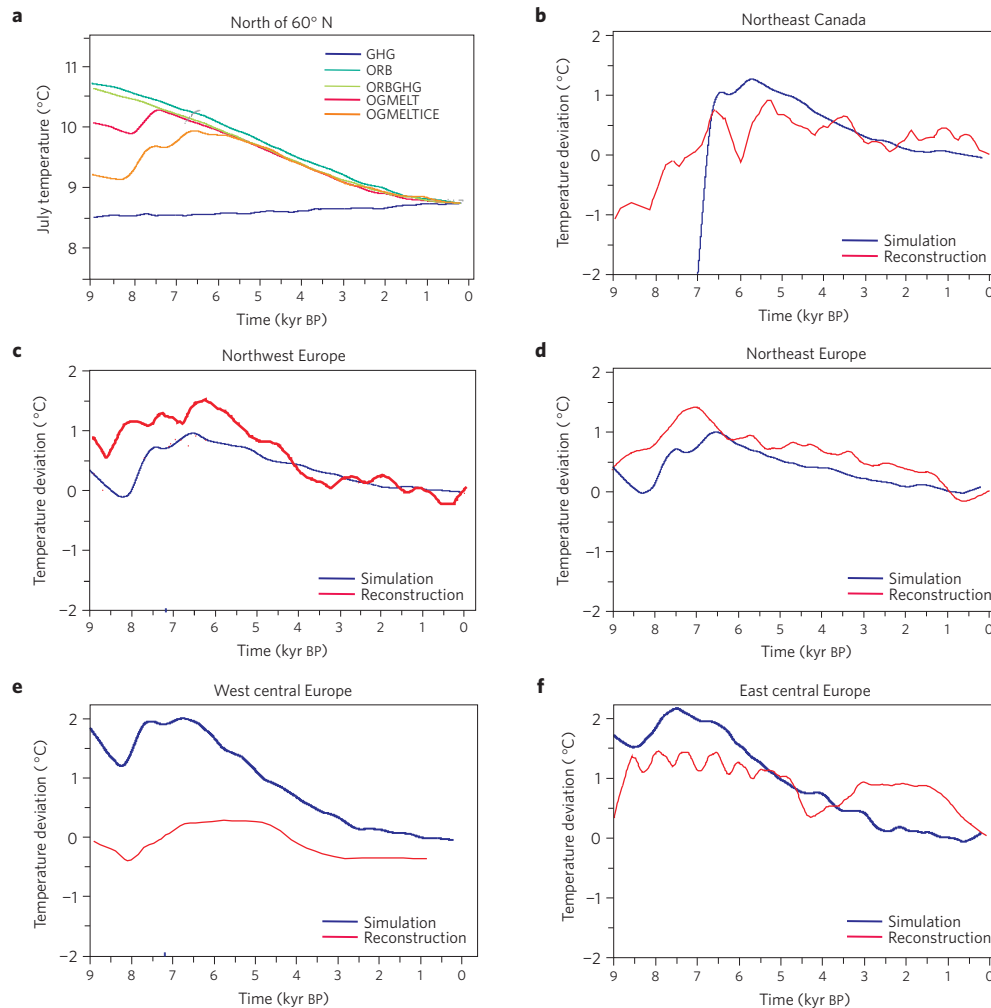


Figure 1 | Evolution of summer temperature according to model simulations and proxy-based reconstructions. **a**, Model-based absolute July temperatures averaged over the area north of 60° N for different experiments (see Table 1). **b–f**, Simulated and reconstructed July temperatures for different sectors (the reconstructed parameter for **f** is summer (May–August) temperature). The reconstructed curve in **e** is based on one record, potentially explaining part of the model–data difference. Simulated values are shown as deviations from the preindustrial mean and reconstructed values as deviations from the mean of the past 200 years. All temperature curves are smoothed using a locally weighted regression smoother (LOESS) (see Supplementary Information).

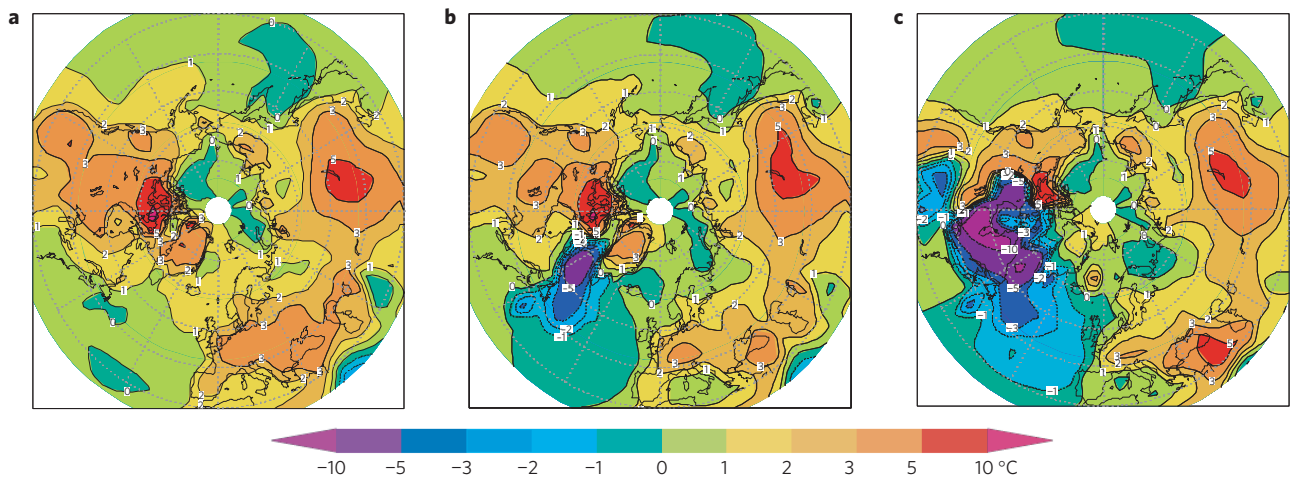


Figure 2 | Simulated early Holocene summer temperatures. **a–c**, July 9–0 kyr BP temperature anomaly for experiments ORBGHG (**a**), OGMELT (**b**) and OGMELTICE (**c**) in the Northern Hemisphere mid- and high latitudes. The difference between the results for OGMELT and ORBGHG reveals the impact of the LIS background meltflux on the early Holocene summer climate, and the difference between OGMELTICE and OGMELT shows the influence of the LIS surface albedo and elevated topography.

As expected, the effect of LIS surface albedo and topography is especially strong over the ice sheet itself, where July temperatures are more than 10 °C lower in OGMELTICE than in ORBGHG (Fig. 2c). However, the North Atlantic Ocean surface is also up to 2 °C cooler in OGMELTICE than in OGMELT, even influencing July temperatures in western Europe (1 °C lower). The LIS cooling effect in OGMELTICE produces a thicker and more extensive Labrador Sea ice cover compared with OGMELT. In OGMELTICE, this sea-ice cover lasts until the LIS has disappeared, causing stratification in the Labrador Sea and preventing deepwater formation here until 7 kyr BP. However, outside the Labrador Sea region, deep convection in OGMELTICE already intensifies after the background meltflux is greatly reduced at 7.8 kyr BP (see Supplementary Information), leading to a stronger meridional overturning circulation and intensified northward ocean heat transport (0.26 PW at 20° S between 7.8 and 7 kyr BP). Thus, the two-stage structure in the Arctic temperature evolution of OGMELTICE (Fig. 1a) is characterized by a first warming phase associated with a strengthening of northward ocean heat transport at 7.8 kyr BP when the main LIS background meltwater flux stops, and a second warming step around 7 kyr BP when the LIS has vanished and deepwater formation starts in the Labrador Sea.

Comparison of the spatio-temporal pattern of peak warming in ORBGHG and OGMELTICE clearly shows where the cooling influence of the LIS is experienced (Fig. 3a, b). The timing of peak warming is similar in both experiments in Alaska, northwest Canada, southeast Europe and in Eurasia south of 45°–50° N, thus showing no significant effect of the LIS, and suggesting that summer temperatures are controlled here by orbital forcing throughout the Holocene. Elsewhere, peak warming is considerably delayed by the LIS. In northeast Canada, peak summer warming is between 7 and 6 kyr BP, thus as expected coinciding with the disappearance of the LIS. Over central Greenland, maximum summer warmth is earlier (8–7 kyr BP) than in southern and northern Greenland (7–5 kyr BP). Along the Atlantic seaboard of Europe, peak warming is clearly delayed by 2 millennia until 7–6 kyr BP, whereas further inland on the Eurasian continent between 40° and 60° N, maximum summer warmth is mostly between 8 and 7 kyr BP. Over areas with perennial sea-ice cover, and also some ocean surfaces, no clear HTM is simulated in July temperatures. Note that here the HTM is most clearly expressed in autumn owing to the thermal inertia of the oceans.

The differences in HTM timing in Eurasia are related to both the distance from the Atlantic coast and the latitudinal position. The LIS produces relatively cold surface-ocean conditions over the northeast Atlantic extending in an eastern direction towards western Europe (that is, 2–4 °C cooler at 9 kyr BP in OGMELTICE than in ORBGHG, Fig. 2). Over the North Atlantic Ocean, the dominant westerly winds are stronger in OGMELTICE compared with ORBGHG (more than 1 m s⁻¹ difference at 9 kyr BP, see Supplementary Information) and the core has shifted eastwards, effectively transporting cold air in summer from the LIS region and the cold North Atlantic to western Europe. Further inland throughout the Eurasian continent, we find at latitudes positioned directly downwind from the area with strongest cooling (that is, between 45° and 60° N) that the HTM is still considerably later (about 1,000 years) than south of this influence where orbital forcing dominates throughout the past 9,000 years (Fig. 3).

Comparison of the model results with proxy-based reconstructions provides support for our inferences about the relative influences of orbital forcing and LIS deglaciation on the circumpolar climate during the Holocene. The higher centennial-scale variability in most reconstructed curves (Fig. 1b–f) compared with the model results is probably related to the influence of centennial-scale forcings (such as solar activity and catastrophic freshwater pulses) not included in the simulations. Our model has captured well the spatio-temporal HTM complexity in North

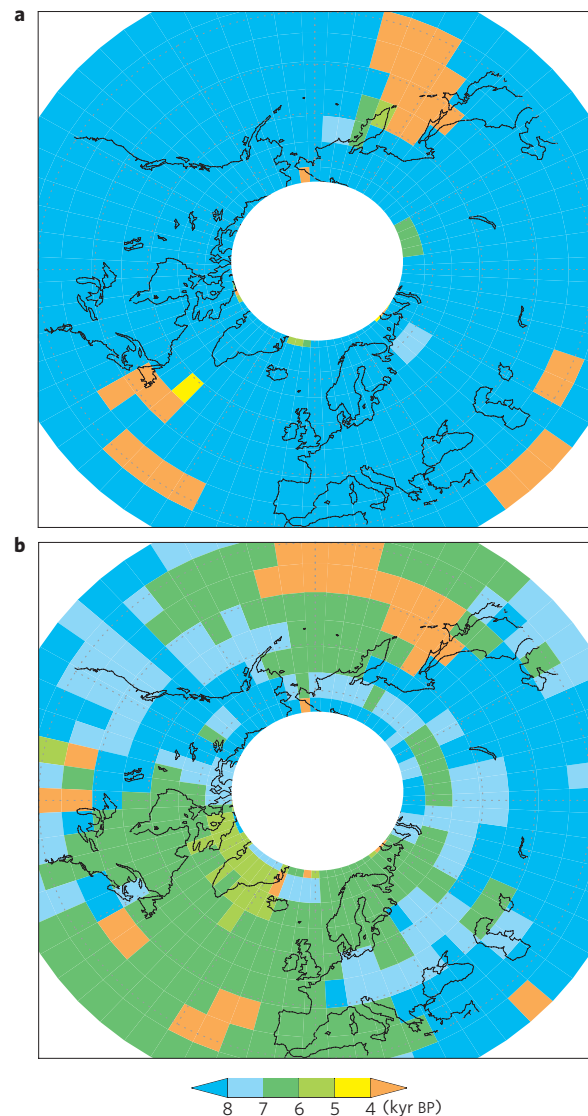


Figure 3 | Simulated HTM timing. a–b, Timing of the maximum July temperature (499-yr running mean) in experiments ORBGHG (a) and OGMELTICE (b). The part of the Arctic Ocean that is perennially covered by sea ice has been masked white. The difference between the two panels shows that the LIS delays peak HTM warming by up to 2,000 years over the North Atlantic Ocean, its seaboard and over the Eurasian continent in a belt between 40°–60° N. South of this belt and in northwest North America, orbital forcing dominates, resulting in an early Holocene HTM timing in concordance with the summer insolation maximum.

America found in data⁴, suggesting that the area west of the LIS (Alaska and northwest Canada) experienced warmest conditions early in the Holocene (before 9 kyr BP), in line with orbital forcing. In contrast, proxy data show that the LIS delays the HTM until 7 kyr BP in the area of the remnant LIS (northeast Canada). This is also seen in our simulated regional July temperature for northeast Canada (Fig. 1b). The modelled HTM timing agrees with reconstructions for this region, although these suggest less extreme changes than our model (Fig. 1b). The simulated delayed warming in southern and northern Greenland compared with central Greenland is also seen in ice cores^{17,18}.

Detailed comparison with quantitative reconstructions of July and summer temperatures in Europe (Fig. 1c–f) also reveals distinct similarities concerning key aspects of Holocene climate evolution, such as the relatively cool early Holocene (before 8 to 7.5 kyr BP),

the timing of the HTM and the orbitally induced cooling trend after the HTM. In both the model and the data, the summers before 8 to 7.5 kyr BP were 0.5 to 1.0 °C below the HTM level and show similar warming rates towards the HTM onset, confirming an important influence of the LIS deglaciation on the European summer climate. The modelled timing of HTM in Europe falls approximately between 8 and 5 kyr BP, and compares fairly well with the reconstructions, although the data for central European sectors suggest a less pronounced, longer HTM than simulated by our model (Fig. 1e, f). The simulated duration of the HTM is around 2,000 years throughout Europe (Fig. 1c–f). The orbitally induced cooling trend after the peak warming at 5 kyr BP is well captured in the simulations.

A crucial assumption behind our modelling experiments is that the applied LIS forcing is reasonable, as it determines to a large extent the simulated timing of the HTM in Europe. The uncertainty in LIS forcing is relatively large compared with the uncertainty in orbital and greenhouse forcings, which are both quite well established. In our simulations, we assumed that the LIS had vanished by about 7 kyr BP as suggested by Peltier¹⁰. Recent data confirm that significant LIS melting lasted only until 6.8 kyr BP, although small icecaps seem to have persisted in northern Quebec and Labrador until 6 kyr BP (ref. 12). We based the amount of LIS meltwater released on published estimates¹⁹. We have not extensively tested the sensitivity of our early Holocene state to different background meltwater fluxes to evaluate the impact of the uncertainty in LIS freshwater forcing. However, note that the resulting ocean circulation is consistent with palaeoceanographic reconstructions, with enhancement of the overturning strength after ~8 kyr BP (ref. 20) and initiation of deep convection in the Labrador Sea^{21,22} around 7 kyr BP. We thus assume that our LIS forcing represents a reasonable approximation.

To summarize, here we present climate model results revealing consistently with proxy records that the complex spatio-temporal structure of the HTM in the circumpolar Northern Hemisphere can be explained by interplay between orbital-induced summer insolation and the disintegrating LIS. Even in northwest and northeast Europe and on the Eurasian continent far from the Atlantic coast, peak warmth associated with the HTM was delayed by up to 2,000 years owing to the LIS cooling effect. Our results clearly show that warm climates are sensitive to relatively minor changes in ice-sheet configuration. This implies that it is important to consider transient ice–climate interactions when studying climate response during periods of warming.

Methods

The model simulations were carried out with the ECBilt–CLIO–VECODE coupled global climate model for the period 9–0 kyr BP. ECBilt–CLIO–VECODE has been successfully applied in several palaeoclimatic studies, simulating climates that compare favourably with proxy-based reconstructions, for instance for the last glacial maximum²³, the 8.2 kyr event²⁴ and the last millennium²⁵. This shows that the model is a valuable tool in palaeoclimate studies. However, it is important to note that our model has an intermediate complexity and that particularly the atmospheric component ECBilt has simplified dynamics and low spatial resolution compared with comprehensive general circulation models. This limits a detailed simulation of the atmospheric circulation, with possible consequences for the atmospheric flow over the LIS and spatial details of the surface temperature anomalies. Details on the model and experimental design are provided in Supplementary Information.

The proxy-based temperatures are based on selected quantitative reconstructions from fossil pollen, chironomid and diatom records preserved in lake sediments. Detailed information on the applied reconstruction technique and data sources are provided in Supplementary Information.

Received 4 February 2009; accepted 6 April 2009;
published online 3 May 2009

References

1. Wanner, H. *et al.* Mid- to late Holocene climate change: An overview. *Quat. Sci. Rev.* **27**, 1791–1828 (2008).
2. Jansen, E. *et al.* in *Climate Change 2007: The Physical Science Basis. 4th Assessment Report IPCC* (eds Solomon, S. *et al.*) 433–498 (Cambridge Univ. Press, 2007).

3. Jansen, E. *et al.* in *Natural Climate Variability and Global Warming: A Holocene Perspective* (eds Battarbee, R. W. & Binney, H. A.) 123–137 (Wiley–Blackwell, 2008).
4. Kaufman, D. S. *et al.* Holocene thermal maximum in the western Arctic (0–180° W). *Quat. Sci. Rev.* **23**, 529–560 (2004).
5. Rimbu, N. *et al.* Holocene climate variability as derived from alkenone sea surface temperature and coupled ocean–atmosphere model experiments. *Clim. Dyn.* **23**, 215–227 (2004).
6. Renssen, H. *et al.* Simulating the Holocene climate evolution at northern high latitudes using a coupled atmosphere–sea ice–ocean–vegetation model. *Clim. Dyn.* **24**, 23–43 (2005).
7. Wiersma, A. P. *et al.* Evaluation of different freshwater forcing scenarios for the 8.2 ka BP event in a coupled climate model. *Clim. Dyn.* **27**, 831–849 (2006).
8. Renssen, H., Goosse, H. & Fichefet, T. Contrasting trends in North Atlantic deep-water formation in the Labrador Sea and Nordic Seas during the Holocene. *Geophys. Res. Lett.* **32**, L08711 (2005).
9. Steffensen, J. P. *et al.* High-resolution Greenland Ice Core data show abrupt climate change happens in few years. *Science* **321**, 680–684 (2008).
10. Peltier, W. Global glacial isostasy and the surface of the ice-age Earth: The ICE-5G (VM2) model and GRACE. *Annu. Rev. Earth Planet. Sci.* **32**, 111–149 (2004).
11. Linden, M. *et al.* Holocene shore displacement and deglaciation chronology in Norrbotten, Sweden. *Boreas* **35**, 1–22 (2006).
12. Carlson, A. E. *et al.* Rapid early Holocene deglaciation of the Laurentide ice sheet. *Nature Geosci.* **1**, 620–624 (2008).
13. Kutzbach, J. E. & Webb, T. III. in *Global Climates Since the Last Glacial Maximum* (eds Wright, H. E. Jr *et al.*) 5–11 (Univ. Minnesota Press, 1993).
14. Opsteegh, J. D. *et al.* ECBILT: A dynamic alternative to mixed boundary conditions in ocean models. *Tellus A* **50**, 348–367 (1998).
15. Goosse, H. & Fichefet, T. Importance of ice–ocean interactions for the global ocean circulation: A model study. *J. Geophys. Res.* **104**, 23337–23355 (1999).
16. Brovkin, V. *et al.* Carbon cycle, vegetation and climate dynamics in the Holocene: Experiments with the CLIMBER-2 model. *Glob. Biogeochem. Cycles* **16**, 1139 (2002).
17. Dahl-Jensen, D. *et al.* Past temperatures directly from the Greenland ice sheet. *Science* **282**, 268–271 (1998).
18. Johnsen, S. *et al.* Oxygen isotope and palaeotemperature records from six Greenland ice-core stations: Camp Century, Dye-3, GRIP, GISP2, Renland and NorthGRIP. *J. Quat. Sci.* **16**, 299–307 (2001).
19. Licciardi, J. M. *et al.* in *Mechanisms of Global Climate Change at Millennial Time Scale* (eds Clark, P. U. *et al.*) 177–201 (American Geophysical Union, 1999).
20. Hall, I. R. *et al.* Centennial to millennial scale Holocene climate–deep water linkage in the North Atlantic. *Quat. Sci. Rev.* **23**, 1529–1536 (2004).
21. de Vernal, A. & Hillaire-Marcel, C. Provincialism in trends and high frequency changes in the northwest North Atlantic during the Holocene. *Glob. Planet. Change* **54**, 263–290 (2006).
22. Hillaire-Marcel, C., de Vernal, A. & Piper, D. J. W. Lake Agassiz final drainage event in the northwest North Atlantic. *Geophys. Res. Lett.* **34**, L15601 (2007).
23. Roche, D. M. *et al.* Climate of the last glacial maximum: Sensitivity studies and model–data comparison with the LOVECLIM coupled model. *Clim. Past* **3**, 205–224 (2007).
24. Wiersma, A. P. & Renssen, H. Model–data comparison for the 8.2 ka BP event: Confirmation of a forcing mechanism by catastrophic drainage of Laurentide Lakes. *Quat. Sci. Rev.* **25**, 63–88 (2006).
25. Goosse, H. *et al.* Modelling the climate of the last millennium: What causes the differences between simulations? *Geophys. Res. Lett.* **32**, L06710 (2005).
26. Berger, A. L. Long-term variations of daily insolation and Quaternary climatic changes. *J. Atmos. Sci.* **35**, 2363–2367 (1978).
27. Raynaud, D. *et al.* The ice record of greenhouse gases: a view in the context of future changes. *Quat. Sci. Rev.* **19**, 9–17 (2000).

Acknowledgements

The authors thank M. W. Kerwin for making his data set available for this study.

Author contributions

All authors collaborated on the text. H.R. and D.M.R. designed the model boundary conditions, H.R. carried out the model simulations, and H.R., D.M.R., H.G. and T.F. analysed the climate model results. H.S. and O.H. compiled records for the temperature reconstructions.

Additional information

Supplementary information accompanies this paper on www.nature.com/naturegeoscience. Reprints and permissions information is available online at <http://npg.nature.com/reprintsandpermissions>. Correspondence and requests for materials should be addressed to H.R.